Monodisperse Glassy-Nematic Conjugated Oligomers with Chemically Tunable Polarized Light Emission

Yanhou Geng,[†] Andrew C. A. Chen,[†] Jane J. Ou,[†] and Shaw H. Chen*[,†,§]

Department of Chemical Engineering, and Laboratory for Laser Energetics, Center for Optoelectronics and Imaging, University of Rochester, 240 East River Road, Rochester, New York 14623-1212

Kevin Klubek,[‡] Kathleen M. Vaeth,[||] and Ching W. Tang[‡]

Hard Copy and Display Technology Division, and Imaging Materials Division, Eastman Kodak Company, 1999 Lake Avenue, Rochester, New York 14650-2116

Received July 3, 2003. Revised Manuscript Received September 9, 2003

A novel series of monodisperse conjugated oligomers were synthesized by inserting varied segments into blue-emitting oligofluorenes to complete the color gamut of light emission. Quantum mechanical calculations revealed that the electron transition dipoles lie largely parallel to the long molecular axes of the central segments responsible for light emission. The orientational order parameter characterizing molecular alignment in thermally processed glassy-nematic films was evaluated at 0.77 to 0.87 by UV−vis absorption dichroism. With an emission dichroic ratio ranging from 9.4 to 13.7, polarized photoluminescence provided further evidence that the long molecular axes are aligned with the nematic director. Polarized organic light-emitting diodes (OLEDs) comprising selected materials resulted in red and yellowish green light emission with dichroic ratios of 14.4 and 18.0 and luminance yields of 0.51 and 5.91 cd/A, respectively. These two sets of data represent the best performance to date of red and green polarized OLEDs.

I. Introduction

Polymers with an extended π-conjugation hold promise for electronic and photonic applications, such as thin-film transistors, light-emitting diodes, photovoltaics, and sensors.[1,2] Of particular interest are poly(fluorene)s that have been demonstrated for blue organic light-emitting diodes, OLEDs.[3−5] Linearly polarized blue OLEDs have also been demonstrated by taking advantage of thermotropic nematic mesomorphism.[4−13] Furthermore, modulation of electronic energy levels through copolymerization has been explored for varied emissive colors across the visible region.[3,14−19] Limited progress has been reported on polarized OLEDs other than blue.[20−24] In contrast to conjugated polymers, monodisperse conjugated oligomers are characterized by a well-defined and uniform molecular structure (i.e., chain

* To whom correspondence should be addressed. E-mail: shch@lle.rochester.edu. Fax: (585)273-1014.

[†] Department of Chemical Engineering, University of Rochester.

[‡] Hard Copy and Display Technology Division, Eastman Kodak Company.

[§] Laboratory for Laser Energetics, University of Rochester.

[||] Imaging Materials Division, Eastman Kodak Company.

(1) Hadziioannou, G., van Hutten, P. F., Eds. *Semiconducting Polymers: Chemistry, Physics and Engineering*; Wiley-VCH: Weinheim, 2000.

(2) McQuade, D. T.; Pullen, A. E.; Swager, T. M. *Chem. Rev.* **2000**, *100*, 2537.

(3) Bernius, M. T.; Inbasekaran, M.; O'Brien, J.; Wu, W. *Adv. Mater.* **2000**, *12*, 1737.

(4) Neher, D. *Macromol. Rapid Commun.* **2001**, *22*, 1365.

(5) Scherf, U.; List, E. J. W. *Adv. Mater.* **2002**, *14*, 477.

(6) Grell, M.; Bradley, D. D. C. *Adv. Mater.* **1999**, *11*, 895.

(7) Grell M.; Bradley, D. D. C.; Inbasekaran, M.; Woo, E. P. *Adv. Mater.* **1997**, *9*, 798.

(8) Whitehead, K. S.; Grell, M.; Bradley, D. D. C.; Jandke, M.; Strohriegl, P. *Appl. Phys. Lett.* **2000**, *76*, 2946.

(9) Grell, M.; Knoll, W.; Lupo, D.; Meisel, A.; Miteva, T.; Neher, D.; Nothofer, H.-G.; Scherf, U.; Yasuda, A. *Adv. Mater.* **1999**, *11*, 671.

(10) Miteva, T.; Meisel, A.; Knoll, W.; Nothofer, H.-G.; Scherf, U.; Müller, D. C.; Meerholz, K.; Yasuda, A.; Neher, D. *Adv. Mater.* **2001**, *13*, 565.

(11) Sainova, D.; Zen, A.; Nothofer, H.-G.; Asawapirom, U.; Scherf, U.; Hagen, R.; Bieringer, T.; Kostromine, S.; Neher, D. *Adv. Funct. Mater.* **2002**, *12*, 49.

(12) Yang, X. H.; Neher, D.; Lucht, S.; Nothofer, H.; Güntner, R.; Scherf, U.; Hagen, R.; Kostromine, S. *Appl. Phys. Lett.* **2002**, *81*, 2319.

(13) Jandke, M.; Hanft, D.; Strohriegl, P.; Whitehead, K.; Grell, M.; Bradley, D. D. C. *SPIE Proc.* **2001**, *4105*, 338.

(14) Müller, C. D.; Falcou, A.; Reckefuss, N.; Rojahn, M.; Wiederhirn, V.; Rudati, P.; Frohne, H.; Nuyken, O.; Becker, H.; Meerholz, K. *Nature* **2003**, *421*, 829.

(15) Ego, C.; Marsitzky, D.; Becker, S.; Zhang, J.; Grimsdale, A. C.; Müllen, K.; MacKenzie, J. D.; Silva, C.; Friend, R. H. *J. Am. Chem. Soc.* **2003**, *125*, 437.

(16) Liu, M. S.; Jiang, X.; Liu, S.; Herguth, P.; Jen, A. K.-Y. *Macromolecules* **2002**, *35*, 3532.

(17) Johansson, D. M.; Theander, M.; Granlund, T.; Inganäs, O.; Andersson, M. R. *Macromolecules* **2001**, *34*, 1981.

(18) Lim, E.; Jung, B.-J.; Shim, H.-K. *Macromolecules* **2003**, *36*, 4288.

(19) Liu, B.; Yu, W.-L.; Lai, Y.-H.; Huang, W. *Macromolecules* **2000**, *33*, 8945.

(20) Bolognesi, A.; Botta, C.; Facchinetti, D.; Jandke, M.; Kreger, K.; Strohriegl, P.; Relini, A.; Rolandi, R.; Blumstengel, S. *Adv. Mater.* **2001**, *13*, 1072.

(21) Contoret, A. E. A.; Farrar, S. R.; Jackson, P. O.; Khan, S. M.; May, L.; O'Neil, M.; Nicholls, J. E.; Kelly, S. M.; Richards, G. J. *Adv. Mater.* **2000**, *12*, 971.

(22) Jandke, M.; Strohriegl, P.; Gmeiner, J.; Brütting, W.; Schwoerer, M. *Adv. Mater.* **1999**, *11*, 1518.

(23) Whitehead, K. S.; Grell, M.; Bradley, D. D. C.; Inbasekaran, M.; Woo, E. P. *Synth. Met.* **2000**, *111−112*, 181.

(24) Bolognesi, A.; Bajo, G.; Paloheimo, J.; Östergård, T.; Stubb, H. *Adv. Mater.* **1997**, *9*, 121.

10.1021/cm034579m CCC: $25.00 © 2003 American Chemical Society
Published on Web 10/11/2003

Chart 1. General Structures of Fluorene Based Monodisperse Oligomers

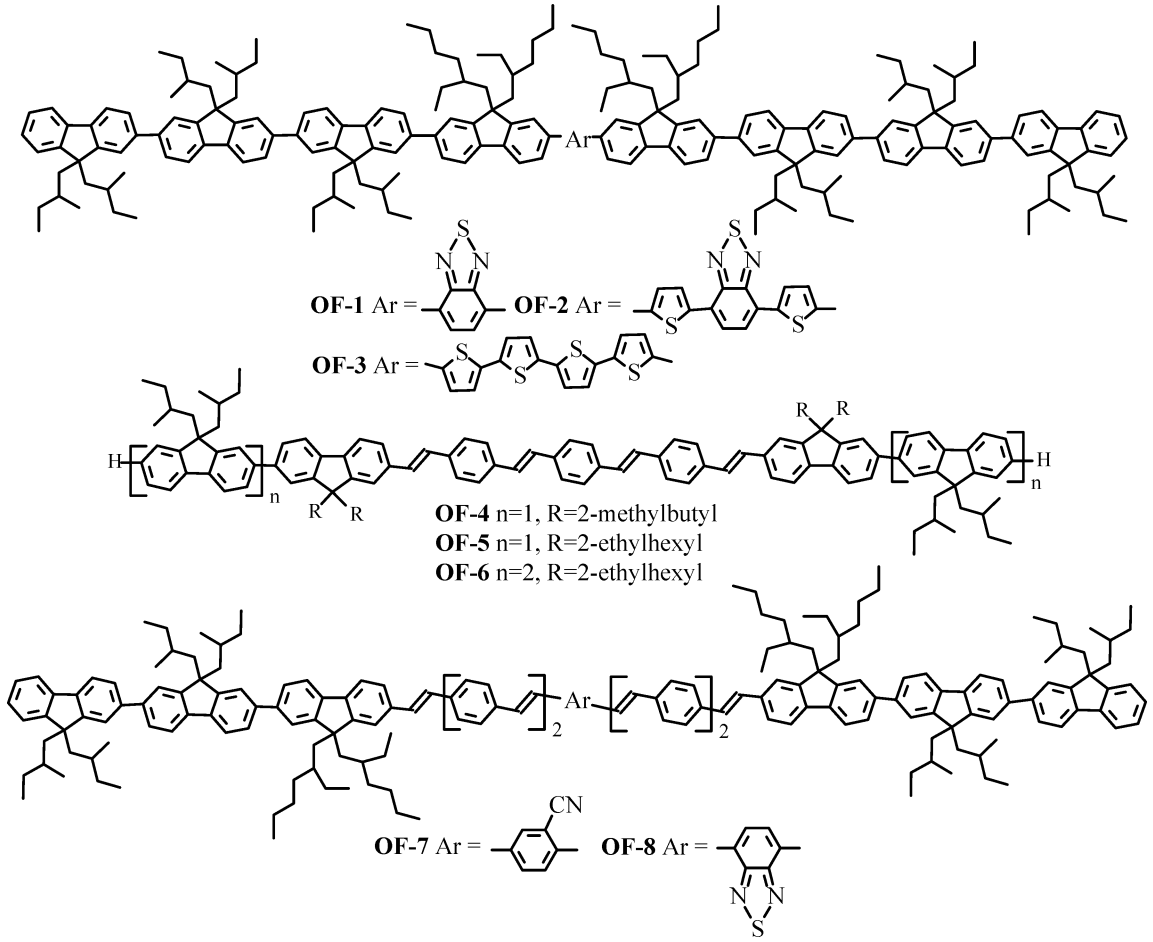

length and comonomer sequence) as well as superior chemical purity (e.g., via recrystallization or column chromatography). These intrinsic features are imperative to furnishing fundamental insight into how chemical structure affects electronic, photonic, and morphological properties. From a practical standpoint, chemical purity and structural uniformity are critical to the performance of OLEDs. Traces of impurity may result in quenching of excitons. In the absence of chain entanglements or defects (e.g., bends and kinks), relatively short and uniform chains are believed to be conducive to the formation of monodomain films. However, oligomers are generally more prone to crystallization than polymers, resulting in polycrystalline films that scatter light and limit charge injection and transport. In this regard, materials capable of glass transition while resisting crystallization are expected to form glassy films without grain boundaries, thus better suited for device application. Few conjugated oligomers have been reported to exhibit thermotropic nematic mesomorphism.[25−27] In a recent paper, a series of monodisperse oligo(fluorene)s have been reported as the first examples of glassy-nematic conjugated oligomers,[28] with which strongly polarized and highly efficient blue OLEDs have also been achieved.[29] The main theme of the present study is on novel monodisperse conjugated oligomers with chemically tunable emissive colors through molecular design assisted by computational chemistry, material synthesis, and OLED device fabrication and characterization.

II. Results and Discussion

To serve as a linearly polarized light-emitter, materials should preferably possess three molecular characteristics: (i) a rodlike molecule with a large aspect ratio; (ii) an electron transition dipole parallel to the long molecular axis; and (iii) the ability to form a monodomain glassy-nematic film across a large area. To achieve these objectives, a series of monodisperse oligo(fluorene)s were demonstrated to be capable of highly efficient blue emission with the strongest polarization ratio ever observed.[28,29] Depicted in Chart 1 are new monodisperse conjugated oligomers designed for polarized full-color emission through chemical modification of previously reported oligo(fluorene)s. The general idea has been explored with fluorene copolymers for emission across the entire visible region.[3,14−19] In the present study, we aimed at monodisperse oligomers comprising a central segment end-capped by di-, tri-, or tetrafluorenes with aliphatic pendants to ensure solubility.

(25) Gill, R. E.; Meetsma, A.; Hadziioannou, G. *Adv. Mater.* **1996**, *8*, 212.
(26) Nierengarten, J.-F.; Guillon, D.; Heinrich, B.; Nicoud, J.-F. *Chem. Commun.* **1997**, 1233.
(27) Schenning, A. P. H. J.; Kilbinger, A. F. M.; Biscarini, F.; Cavallini, M.; Cooper, H. J.; Derrick, P. J.; Feast, W. J.; Lazzaroni, R.; Leclère, Ph.; McDonell, L. A.; Meijer, E. W.; Meskers, S. C. J. *J. Am. Chem. Soc.* **2002**, *124*, 1269.
(28) Geng, Y. H.; Culligan, S. W.; Trajkovska, A.; Wallace, J.; Chen, S. H. *Chem. Mater.* **2003**, *15*, 542.
(29) Culligan, S. W.; Geng, Y. H.; Chen, S. H.; Klubek, K.; Vaeth, K. M.; Tang, C. W. *Adv. Mater.* **2003**, *15*, 1176.

Scheme 1. Synthesis of Monodisperse Oligomers OF-1, OF-2, and OF-3[a]

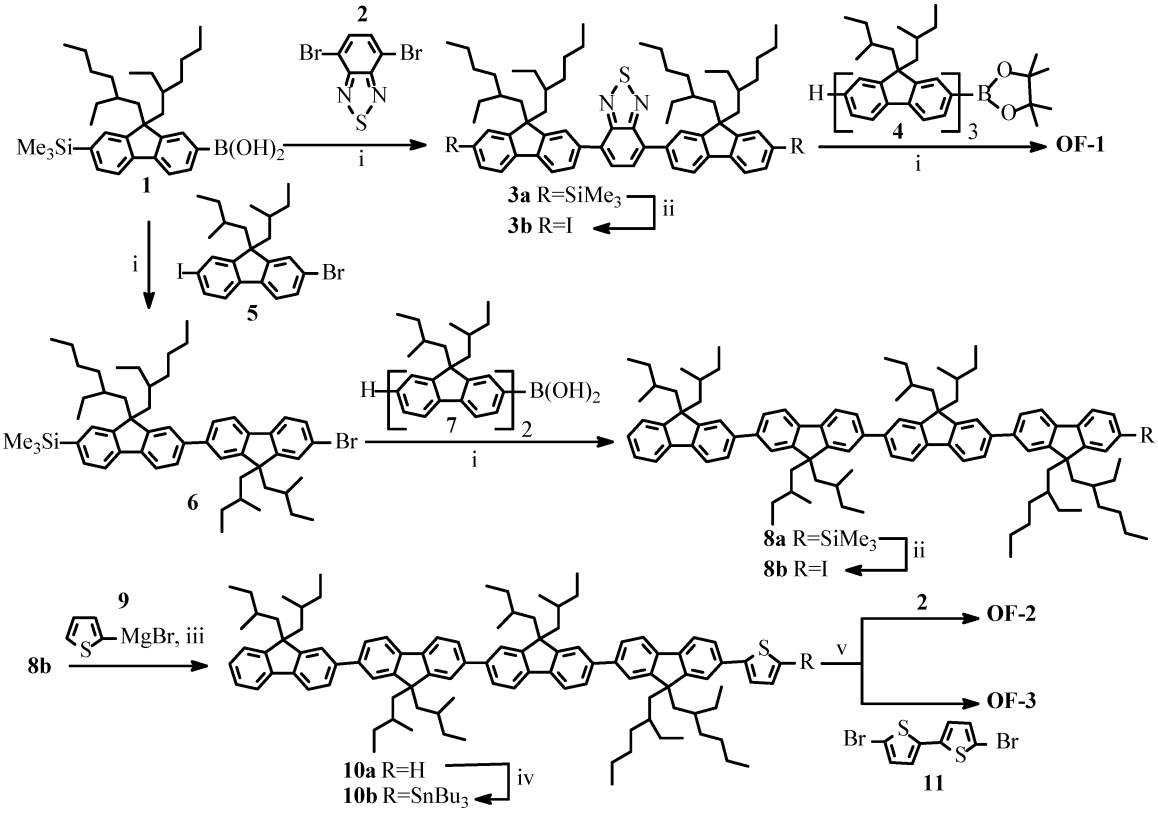

[a] (i) $Pd(PPh_3)_4$, Na_2CO_3 (2.0 M *aq.*), 90 °C. (ii) ICl, 0 °C. (iii) $Pd(dppf)Cl_2$, rt. (iv) (1) *n*-BuLi, 0 °C; (2) Bu_3SnCl, −78 °C to room temperature. (v) $Pd(PPh_3)_4$, 100 °C.

Scheme 2. Synthesis of Monodisperse Oligomers OF-4, OF-5, OF-6, OF-7, and OF-8[a]

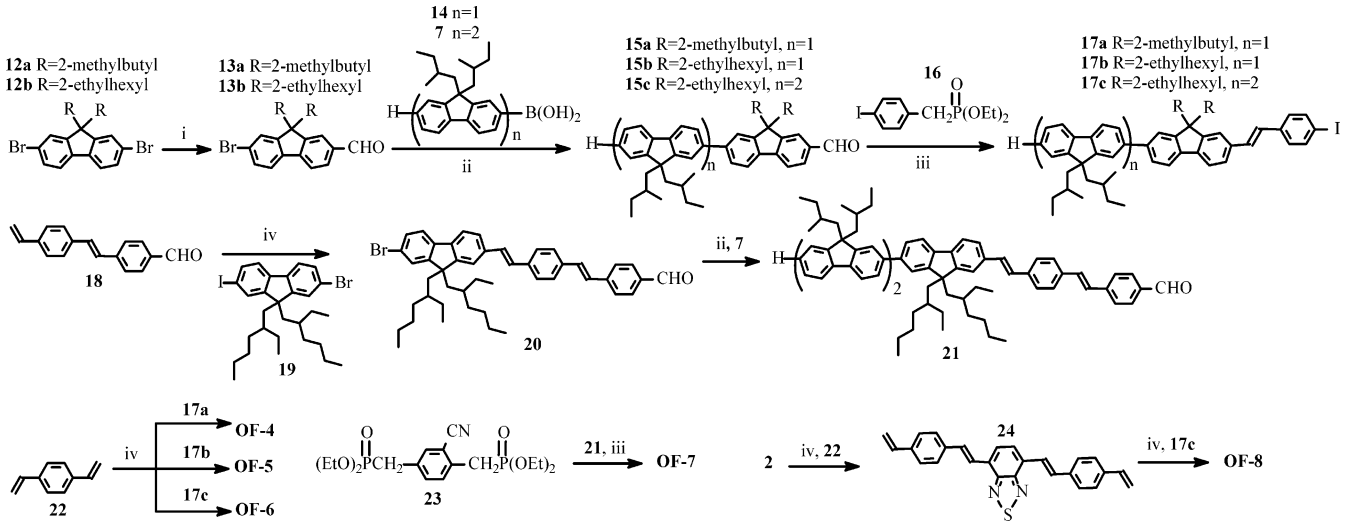

[a] (i) (1) *n*-BuLi, −78 °C; (2) DMF, −78 °C to room temperature. (ii) $Pd(PPh_3)_4$, Na_2CO_3 (2.0 M *aq.*), 90 °C. (iii) KO-*t*-Bu, rt. (iv) $Pd(OAc)_2$/K_2CO_3/Bu_4NBr, 110 °C.

Material synthesis was accomplished following the divergent−convergent approach, as shown in Schemes 1 and 2. On the basis of Scheme 1, **OF-1** was synthesized by Suzuki coupling[30] in a 39% yield, whereas **OF-2** and **OF-3** were synthesized by Stille coupling[31] in yields of 72% and 60%, respectively. According to Scheme 2, **OF-4**, **OF-5**, **OF-6**, and **OF-8** were synthesized by Heck coupling[32] in 64−77% yields, and **OF-7** was synthesized by the Horner−Wadsworth−Emmons (HWE) reaction[33] in a 69% yield. Trace amounts of *cis*-isomers accompanying **OF-4**−**8** were removed with column chromatography to afford pure final products. The molecular structures of **OF-1**−**8** were validated with elemental analysis, and ^1H NMR, and MALDI-TOF mass spectroscopic techniques.

(30) Miyaura, N.; Suzuki, A. *Chem. Rev.* **1995**, *95*, 2457.
(31) Bao, Z.; Chan, W. K.; Yu, L. *J. Am. Chem. Soc.* **1995**, *117*, 12426.
(32) Beletskaya, I. P.; Cheprakov, A. V. *Chem. Rev.* **2000**, *100*, 3009.
(33) Maddux, T.; Li, W.; Yu, L. *J. Am. Chem. Soc.* **1997**, *119*, 844.

Table 1. Phase Transition Temperatures (T_g and T_c), Absorption and Emission Data in Dilute Solution and Neat Film, Orientational Order Parameter (S_{ab}) and Emission Dichroic Ratio (R_{PL}) in Neat Film, and Photoluminescence Quantum Yield in Dilute Solution (Φ_{PL})

				λ_{ab}, nm[c]		λ_{PL}, nm[c]				
compound	T_g[a] (°C)	T_c[a] (°C)	τ[b] (nm)	solution	film	solution	film	S_{ab} (λ_{ab})[d]	R_{PL} (λ_{PL})	Φ_{PL} (%)[e]
OF-1	106	>350	80	364, 421	362, 430	533	533	0.83 (362), 0.87 (430)	12.7 ± 0.8 (533)	77
OF-2	104	304	95	374, 518	374, 534	635	643	0.77 (374), 0.77 (534)	9.8 ± 0.9 (643)	68
OF-3	112	342	72	364, 445	367	520, 558	532, 572	0.79 (367)	12.6 (532) 13.3 (572)	42
OF-4[f]	127	>320	N/A	419	N/A	461, 493	N/A	N/A	N/A	82
OF-5	97	>320	79	421	427	461, 493	479, 512	0.82 (427)	9.7 ± 0.3 (479) 11.7 ± 0.3 (512)	82
OF-6	111	>320	74	421	422	461, 493	479, 511	0.79 (422)	9.4 (479) 11.8 (511)	74
OF-7	110	>320	78	434	432	479, 513	545	0.84 (432)	13.7 ± 1.0 (545)	75
OF-8	116	>320	73	396, 488	400, 504	576	632	0.79 (400), 0.84 (504)	13.2 (632)	47

[a] Transition temperatures gathered from DSC heating scans at 20 °C/min of samples preheated to 350 °C for **OF-1**, **OF-2**, and **OF-3** and 320 °C for other samples followed by cooling at −20 °C/min to −30 °C; T_g represents the inflection point across glass transition, and T_c is the nematic to isotropic transition as identified by polarizing optical microscopy. [b] Film thickness, τ, determined with spectroscopic ellipsometry. [c] Absorption and emission (with unpolarized excitation at 370 nm) spectra in toluene of 10^{-6} to 10^{-7} M, and those of thermally annealed neat films. [d] Orientational order parameter, $S_{ab} = (R_{ab} - 1)/(R_{ab} + 2)$, accompanied by an uncertainty of ±0.02, in which R_{ab} is absorption dichroic ratio. [e] Solution photoluminescence quantum yield at 10^{-6} to 10^{-7} M in toluene with an uncertainty of ±2% using pyrromethene 546 as the standard. [f] No glassy-nematic film could be prepared via thermal annealing without encountering crystallization for further investigation.

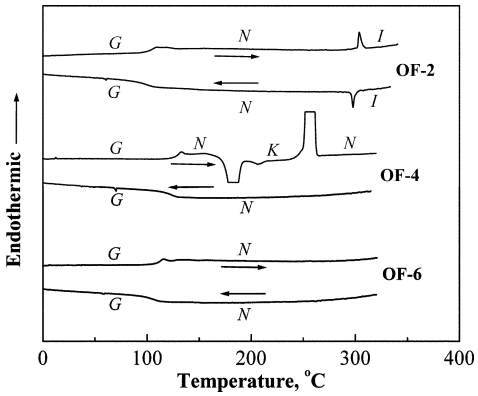

Figure 1. DSC second heating and first cooling scans at ±20 °C/min of a sample of **OF-2** preheated to 350 °C, and samples of **OF-4** and **6** to 320 °C, the upper temperature limits to avoid thermal decomposition, with subsequent cooling at −20 °C/min to −30 °C. Symbols: G, glassy; N, nematic; K, crystalline; I, isotropic.

Thermotropic properties characterized by differential scanning calorimetry and hot-stage polarizing optical microscopy are summarized in Table 1. For these two types of analysis, the samples were preheated to 350 °C for **OF-1**−**3** and 320 °C for **OF-4**−**8**, the upper temperature limits to avoid thermal decomposition, with subsequent cooling at −20 °C/min to −30 °C. Representative results from the first cooling and the second heating scans at ±20 °C/min are reproduced in Figure 1. With a glass transition but no tendency to recrystallization on heating or cooling, **OF-2** and **6** are well suited for the preparation of monodomain glassy-nematic films through thermal processing. The uniaxial molecular alignment characteristic of a nematic liquid crystal can be frozen in the solid state on cooling to below glass transition temperature, T_g, without encountering crystallization. In contrast, **OF-4** tends to form a polycrystalline film on thermal annealing that scatters light, thus limiting its practical application. All the other samples behave similarly to **OF-2** or **6**, as indicated by the observed T_g and clearing temperature, T_c (see Table 1). Two observations are worth noting with respect to how structure affects solid morphology. With two sets of the 2-methylbutyl pendant replaced by 2-ethylhexyl, the improved ability of **OF-5** over **OF-4** to suppress crystallization is demonstrated. Moreover, adding one more fluorene unit to both ends of **OF-5** led to an increased T_g by 14 °C in **OF-6**.

Light absorption and photoluminescence were characterized for all conjugated oligomers in toluene at 10^{-6} to 10^{-7} mol/L to prevent molecular aggregation. The peak wavelengths, λ_{ab} and λ_{PL}, presented in Table 1 demonstrate the tunability of absorption and emission peak wavelengths via chemical modification. The photoluminescence spectra were found to be independent of the excitation wavelength ranging from 370 to 450 nm with **OF-1** and **3**−**7** and from 370 to 500 nm with **OF-2** and **8**, suggesting that the light-emitting species consist of the central segments of oligomers thanks largely to intramolecular energy transfer. The central *p*-phenylenevinylene segment in conjugation with the terminal di- and trifluorene resulted in identical dilute solution spectra of **OF-4**−**6**. Of particular interest is the ability to tune emission color from blue, viz. that of previously reported oligo(fluorene),[28] across the entire visible region through chemical modification. The photoluminescence quantum yield measured with Pyrromethene 546 as the standard was found to vary from 47 to 82% without a correlation with molecular structure. With the exception of **OF-4**, which tends to crystallize on heating, all conjugated oligomers were used to prepare glassy-nematic films by spin coating from 1.8 wt % toluene solutions onto fused silica substrates containing a buffed poly(3,4-ethylenedioxythiophene)/polystyrene sulfonic acid [PEDOT/PSS] alignment layer. After vacuum-drying, the pristine films were thermally annealed under argon at 10−15 °C above T_g for 25−30 min before cooling to room temperature. Under polarizing optical microscopy, the resultant monodomain glassy-nematic films presented a uniform and textureless (i.e., blank) image but were optically anisotropic. The absence of microcrystallinity on thermal annealing was further validated by electron diffraction (included as the inset in Figure 3).

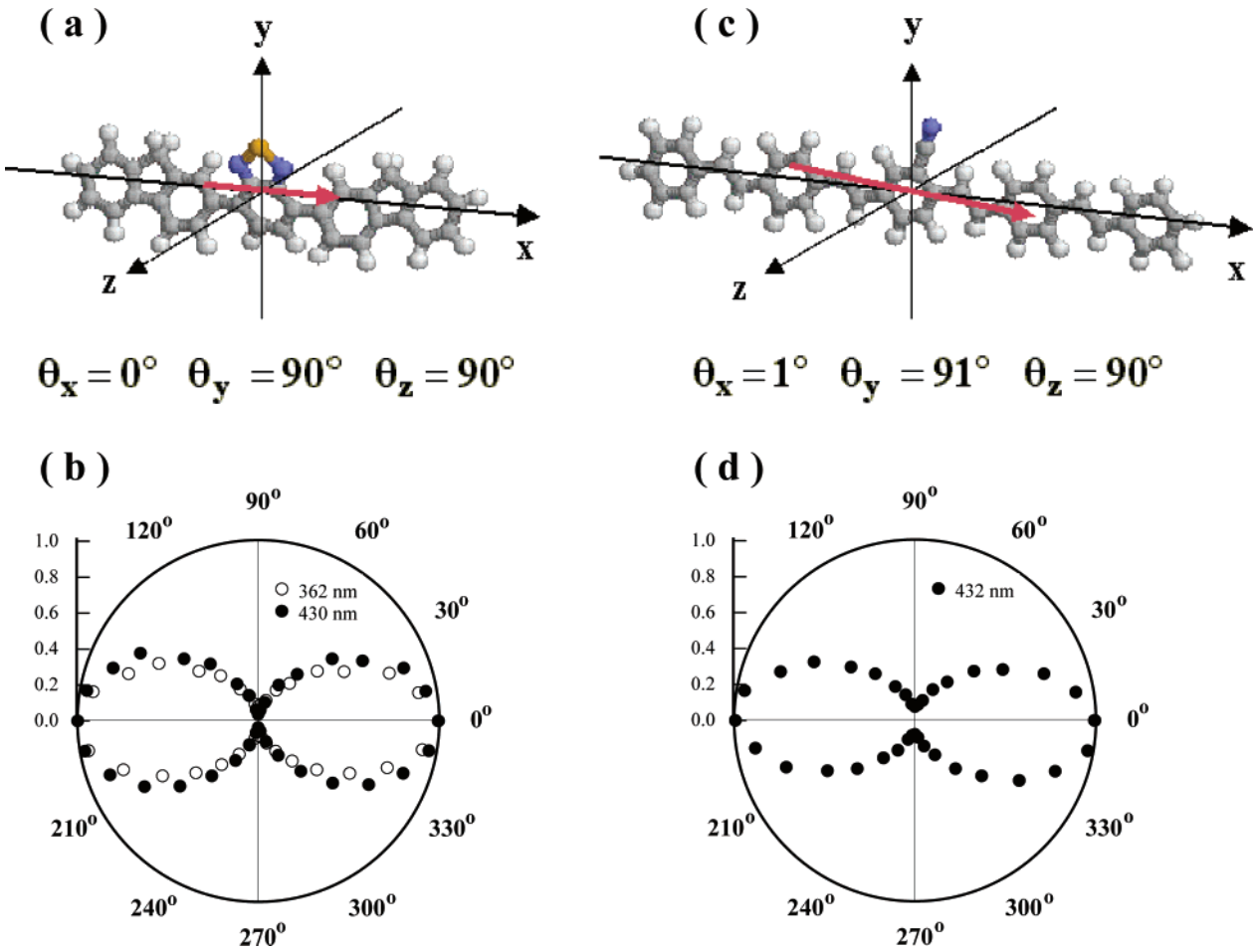

Figure 2. Quantum mechanical calculations based on density functional theory, with the B3LYP functional and the 6-31G(d) basis set, performed using the Gaussian 98 software package to locate electron transition dipoles of the central segments of (a) **OF-1**, and (b) **OF-7**; and UV−vis absorption dichroism at absorption peak wavelengths of glassy-nematic films of (c) **OF-1** and (d) **OF-7**, indicating that the central segments responsible for absorption are aligned with the nematic director placed along 0 and 180° in the polar coordinates.

In general, the neat film's UV−vis absorption showed an appreciable spectral modification compared to dilute solution except for **OF-1**−**3** (see Supporting Information). The spectral modification in photoluminescence is less pronounced (see Supporting Information), but the relatively large red shift observed in neat films of **OF-7** and **8**, as revealed in Table 1, seems to suggest intermolecular interaction or exciton migration to the more planar portion of the molecular structure. The film thickness measured with ellipsometry was found to vary from 72 to 95 nm. Quantum mechanical calculations based on density functional theory, with the B3LYP functional and the 6-31G(d) basis set, were performed using the Gaussian 98 software package to locate electron transition dipoles of the central segments. These transition dipoles were found to lie largely parallel to the long axes of the central segments in all conjugated oligomers, as illustrated in Figure 2 for **OF-1** and **7** with a 2,1,3-benzothiadiazolyl and 2-cyanophenyl group, respectively. The experimental characterization of intermolecular packing between conjugated oligomers remains a major challenge at the present time. Nonetheless, UV−vis absorption dichroism at absorption peak wavelengths of aligned films of **OF-1** and **7** revealed that the central segments responsible for absorption are indeed aligned with the nematic director, placed along 0 and 180° in the polar coordinates shown in Figure 2. Note that the nematic director is defined by the direction in which the PEDOT/PSS-coated substrates were mechanically buffed. The orientational order parameter, S_{ab}, was calculated using the formula, $S_{ab} = (R_{ab} - 1)/(R_{ab} + 2)$, in which R_{ab} is the absorbance parallel over that perpendicular to the nematic director. The values compiled in Table 1 range from 0.77 to 0.87, indicating a high degree of uniaxial molecular alignment. The observed values for the photoluminescence dichroic ratio, R_{PL} at λ_{PL}, range from 9.4 to 13.7 with a trend in qualitative agreement with the observed S_{ab} at λ_{ab}.

Three representative conjugated oligomers, **OF-1**, **OF-2**, and **OF-6**, were selected for the fabrication of linearly polarized organic light-emitting diodes, LPOLEDs, with a device configuration depicted in Figure 3a. Glassy-nematic films were prepared on ITO-patterned substrates following the same procedures as used on fused silica substrates. The film thickness was confirmed by UV−vis absorbance to be identical to the values reported in Table 1 within experimental error. The electroluminescence spectra are reproduced in Figure 3b, in which a LPOLED containing blue-emitting dodecafluorene, viz. **F(MB)10F(EH)2**, in the same device structure[29] is included to complete the color gamut. Specifically, a 73-nm thick film was found to emit nearly pure blue light characterized by the Com-

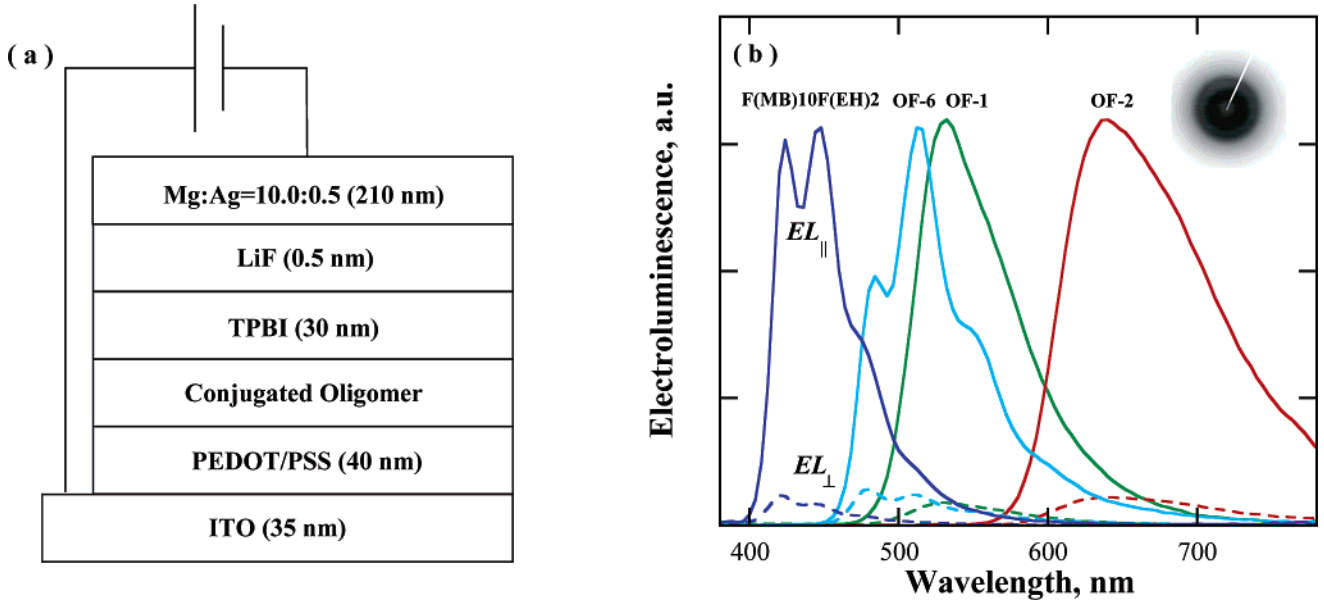

Figure 3. (a) Device structure of the polarized OLEDs prepared for this study; and (b) polarized electroluminescence spectra of devices containing glassy-nematic films of dodecafluorene, **F(MB)10F(EH)2**,[29] **OF-1**, **2**, and **6**, where $EL_{\parallel}$ and $EL_{\perp}$ represent the emitted intensity parallel and perpendicular to the nematic director, respectively. Electron diffraction image included as inset to show the absence of microcrystallinity.

Table 2. OLED Device[a] Performance Data at a Current Density of 20 mA/cm²

compound[b]	voltage (V)	brightness (cd/m²)	yield (cd/A)	R_{EL} (λ_{max})	R_{EL} (integrated)	CIE (x,y)[c]
OF-1	7.9 ± 0.2	1181 ± 30	5.91 ± 0.15	18.0 ± 0.6 (532)	16.0 ± 0.5	(0.363, 0.599)
OF-2	7.5 ± 0.1	101 ± 7	0.51 ± 0.03	14.4 ± 0.4 (636)	13.8 ± 0.4	(0.673, 0.324)
OF-6	9.8 ± 0.2	79 ± 1	0.40 ± 0.01	13.0 ± 0.3 (512)	10.1 ± 0.1	(0.260, 0.536)

[a] Device structure, ITO/PEDOT:PSS/OF/TPBI/LiF/Mg:Ag, containing spin-cast films thermally annealed at 10−15 °C above T_g under argon for 25 to 30 min. [b] Film thickness verified with UV−vis absorbance to be identical to those reported in Table 2. [c] CIE coordinates accompanied by an uncertainty of ±0.001.

mission Internationale de l'Eclairage (CIE) coordinates of (0.159, 0.079), close to the NTSC standard blue, (0.148, 0.080), with a peak polarization ratio of 17 and a luminance yield of 1.10 cd/A.[29] Device performance data at a current density of 20 mA/cm² are presented in Table 2. Note the consistently higher polarization ratio in electroluminescence compared to photoluminescence in **OF-1** and **OF-2** (see Tables 1 and 2), presumably because the former occurs near the buffed PEDOT/PSS alignment layer where a higher degree of molecular alignment prevails, while the latter occurs across the film thickness. However, the electroluminescence spectra largely overlap with photoluminescence from neat films (see Supporting Information). The CIE coordinates, (0.673, 0.324), indicate that **OF-2** produced nearly pure red. Both **OF-1** and **6** produced yellowish green, (0.363, 0.599) and (0.260, 0.536), respectively. That the luminance yield of **OF-1** is more than 14 times that of **OF-6** may be attributed to the fact that the former is more robust than the latter with respect to air exposure, as shown for a poly(*p*-phenylenevinylene);[34] intermolecular interaction could be another reason for the diminished yield with **OF-6**.

Figure 4 delineates how current density and luminance vary with the applied voltage. A turn-on voltage of less than 5 V is noted for the deep red device comprising **OF-2** and the yellowish green device comprising **OF-1** with luminance yields of 0.51 and 5.91 cd/A, respectively, without polarization analysis at a current density of 20 mA/cm². In both cases, the luminance yield stays fairly constant at a current density up to 100 mA/cm². To the best of our knowledge, these are the most efficient and the brightest polarized green and red OLEDs to date.[20−24] The peak polarization ratio of 18.0 observed with **OF-1** is higher than all that have been reported to date in the green region using poly(*p*-phenylenevinylene)s,[22] a fluorene-benzothiadiazole copolymer, and cross-linkable fluorene-thiophene cooligomer.[21,23] The red LPOLEDs that have been reported previously[20,22] exhibited a polarization ratio of 3, which is much lower than the 14.4 achieved with **OF-2**.

III. Conclusions

By inserting varied segments into the previously reported blue-emitting oligo(fluorene)s, a novel series of monodisperse conjugated oligomers were synthesized and characterized to emit visible light across the visible region. Linearly polarized OLEDs were fabricated and characterized using selected materials. The main observations emerging from this study are summarized as follows.

(1) All the oligomers were found to display thermotropic nematic mesomorphism with a glass transition temperature between 97 and 127 °C and a nematic-to-isotropic transition temperature well above 300 °C. With the exception of **OF-4**, all oligomers were processed into monodomain solid films via spin coating and thermal annealing at 10−15 °C above glass transition temper-

(34) Halim, M.; Samuel, I. D. W.; Rebourt, E.; Monkman, A. P. *Synth. Met.* **1997**, *84*, 951.

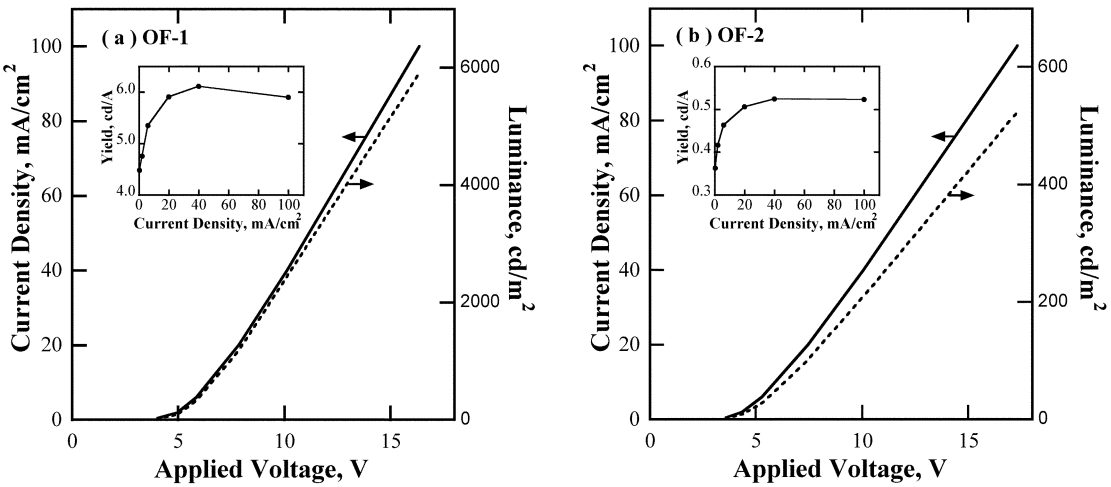

Figure 4. Luminance and current density as functions of applied voltage determined for polarized OLEDs containing glassy-nematic films of (a) **OF-1** and (b) **OF-2** with the insets showing the relationship between luminance yield and current density.

ature for 25−30 min followed by cooling to room temperature.

(2) The uniaxially aligned films showed an orientational order parameter ranging from 0.77 to 0.87, as determined by UV−vis absorption dichroism. Linear polarization analysis of photoluminescence resulted in a ratio ranging from 9.4 to 13.7 with a trend in qualitative agreement with the observed orientational order parameter.

(3) Quantum mechanical calculations based on density functional theory using the Gaussian 98 software package revealed that the electron transition dipoles of the oligomers' central segments lie largely parallel to the long molecular axes, which in turn follow the nematic director defined by mechanically buffing the PEDOT/PSS-coated substrates.

(4) At a current density of 20 mA/cm^2, the OLEDs comprising glassy-neamtic films of **OF-2** and **1**, were found to emit nearly pure red and yellowish green with peak polarization ratios of 14.4 and 18.0, and luminance yields of 0.51 and 5.91 cd/A, respectively. These are the most efficient and the brightest polarized red and green OLEDs with the highest polarization ratio observed to date.

IV. Experimental Section

Material Synthesis. All chemicals, reagents, and solvents were used as received from commercial sources without further purification except tetrahydrofuran (THF) and toluene that had been refluxed over sodium/benzophenone and sodium, respectively, and then distilled before use. Synthesis of intermediates **1**, **4**, **7**, and **14** has been reported elsewhere.[28] Intermediates **16**, **18**, and **23** were synthesized according to literature procedures.[35−37] Synthesis of the rest of the intermediates is included in the Supporting Information.

4,7-Bis[9,9-bis(2-ethylhexyl)-9′,9′,9″,9″,9‴,9‴-hexakis-(2-methylbutyl)-7,2′;7′,2″;7″,2‴-tetrafluoren-2-yl]-2,1,3-benzothiadiazole (OF-1). Into a mixture of **3b** (0.320 g, 0.245 mmol), 2-[9,9,9′,9′,9″,9″-hexakis(2-methylbutyl)-7,2′;7′,2″-terfluoren-2-yl]-4,4,5,5-tetramethyl[1,3,2]dioxaborolan (**4**, 0.600 g, 0.576 mmol) and Pd(PPh$_3$)$_4$ (15 mg, 1.30 × 10^{-2} mmol) were added toluene (6.0 mL) and 2.0 M Na_2CO_3 aqueous solution (4.0 mL, 8.0 mmol). The reaction mixture was stirred at 90 °C for 2 d. When the reaction mixture cooled to room temperature, methylene chloride (30 mL) was added. The organic layer was separated and washed with brine for drying over $MgSO_4$. After the solvent was evaporated off, the residue was purified with column chromatography on silica gel with petroleum ether/methylene chloride (3:1 and then 2:1) as the eluent to yield **OF-1** (0.260 g, 39%) as a yellow solid. ^{1}H NMR (400 MHz, $CDCl_3$): δ (ppm) 8.05−8.13 (m, 4H), 7.95 (d, J = 7.89 Hz, 2H), 7.90 (s, 2H), 7.83−7.89 (m, 10H), 7.82 (d, J = 8.07 Hz, 2H), 7.77 (d, J = 7.32 Hz, 2H), 7.62−7.75 (m, 24H), 7.29−7.49 (m, 6H), 2.12−2.32 (m, 20H), 1.90−2.02 (m, 12H), 0.52−1.02 (m, 132H), 0.30−0.48 (m, 36H). Molecular weight calcd for $C_{202}H_{252}N_2S$: 2740.3. MALD/I TOF MS (dithranol) m/z ([M]$^+$): 2739.9. Anal. Calcd for $C_{202}H_{252}N_2S$: C, 88.54; H, 9.27; N, 1.02; S, 1.17. Found: C, 88.54; H, 8.88; N, 1.01.

4,7-Bis[5-(9,9-bis(2-ethylhexyl)-9′,9′,9″,9″,9‴,9‴-hexakis-(2-methylbutyl)-7,2′;7′,2″;7″,2‴-tetrafluoren-2-yl)-thien-2-yl]-2,1,3-benzothiadiazole (OF-2). Into a degassed mixture of **10b** (1.10 g, 0.657 mmol), **2** (0.0650 g, 0.221 mmol), and Pd(PPh$_3$)$_4$ (20 mg, 1.73 × 10^{-2} mmol) was added toluene (5.0 mL). The mixture was stirred at 100 °C for 2 days. When the reaction mixture had cooled to room temperature, methylene chloride (30 mL) was added. The solution was washed with brine for drying over $MgSO_4$. When the solvent had evaporated off, the residue was purified with column chromatography on silica gel with petroleum ether/methylene chloride (4:1 then 2:1) as the eluent to yield **OF-2** (0.460 g, 72%) as a red solid. ^{1}H NMR (400 MHz, $CDCl_3$): δ (ppm) 8.20−8.25 (m, 2H), 7.98 (s, 2H), 7.60−7.90 (m, 44H), 7.49−7.55 (m, 2H), 7.29−7.48 (m, 6H), 1.85−2.35 (m, 32H), 0.57−1.10 (m, 132H), 0.30−0.50 (m, 36H). Molecular weight calcd for $C_{210}H_{256}N_2S_3$: 2904.5. MALD/I TOF MS (dithranol) m/z ([M]$^+$): 2904.9. Anal. Calcd for $C_{210}H_{256}N_2S_3$: C, 86.84; H, 8.88; N, 0.96; S, 3.32. Found: C, 86.75; H, 9.14; N, 0.97.

2,5‴-Bis[9,9-bis(2-ethylhexyl)-9′,9′,9″,9″,9‴,9‴-hexakis(2-methylbutyl)-7,2′;7′,2″;7″,2‴-tetrafluoren-2-yl]-5,2′;5′,2″;5″,2‴-quaterthiophene (OF-3). The procedure for the synthesis of **OF-2** was followed to prepare **OF-3** from **10b** and 5,5′-dibromo-2,2′-bithiophene (**11**) as a yellow solid in a 60% yield. ^{1}H NMR (400 MHz, $CDCl_3$): δ (ppm) 7.60−7.88 (m, 44H), 7.29−7.46 (m, 8H), 7.10−7.28 (m, 6H) 1.80−2.40 (m, 32H), 0.57−1.15 (m, 132H), 0.30−0.50 (m, 36H). Molecular weight calcd for $C_{212}H_{258}S_4$: 2934.6. MALD/I TOF MS (dithranol) m/z ([M]$^+$): 2935.0. Anal. Calcd for $C_{212}H_{258}S_4$: C, 86.77; H, 8.86; S, 4.37. Found: C, 86.92; H, 8.93.

1,4-Bis[2-[4-[2-(9,9,9′,9′-tetrakis(2-methylbutyl)-2,2′-bifluoren-7-yl)ethenyl]phenyl]ethenyl]benzene (OF-4). Into a degassed mixture of **17a** (1.20 g, 1.43 mmol), 1,4-diethenylbenzene (**22**, 0.085 g, 0.653 mmol), Pd(OAc)$_2$ (10 mg, 4.45 × 10^{-2} mmol), K_2CO_3 (0.238 g, 1.72 mmol), and tetrabutylam-

(35) Kung, H. F.; Lee, C.-W.; Zhuang, Z.-P.; Kung, M.-P.; Hou, C.; Plössl, K. *J. Am. Chem. Soc.* **2001**, *123*, 12740.
(36) Wang, S.; Oldham, W. J., Jr.; Hudack, R. A., Jr.; Bazan, G. C. *J. Am. Chem. Soc.* **2000**, *122*, 5695.
(37) Eckert, J.-F.; Bourgogne, C.; Nierengarten, J.-F. *Chem. Commun.* **2002**, 712.

monium bromide (0.484 g, 1.50 mmol) was added anhydrous DMF (10 mL). The reaction mixture was stirred at 110 °C for 2 d before being poured into a large amount of water. The solid was collected by filtration and redissolved in methylene chloride. The solution was washed with brine for drying over $MgSO_4$. When the solvent had evaporated off, the residue was purified with column chromatography on silica gel with petroleum ether/chloroform (3:1) as the eluent to yield **OF-4** (0.652 g, 64%) as a yellow solid. ^{1}H NMR (400 MHz, $CDCl_3$): δ (ppm) 7.73−7.83 (m, 6H), 7.50−7.72 (m, 26H), 7.30−7.49 (m, 6H), 7.28 (d, J = 16.4 Hz, 2H), 7.15−7.23 (m, 6H), 2.14−2.35 (m, 8H), 1.90−2.10 (m, 8H), 0.60−1.00 (m, 48H), 0.30−0.50 (m, 24H). Molecular weight calcd for $C_{118}H_{134}$: 1551.0. MALD/I TOF MS (dithranol) m/z ($[M]^+$): 1552.0. Anal. Calcd for $C_{118}H_{134}$: C, 91.30; H, 8.70. Found: C, 91.61; H, 8.74.

1,4-Bis[2-[4-[2-(9,9-bis(2-ethylhexyl)-9′,9′-bis(2-methylbutyl)-2,2′-bifluoren-7-yl)ethenyl]phenyl]ethenyl]benzene (OF-5). The procedure for the synthesis of **OF-4** was followed to prepare **OF-5** from **17b** and **22** as a yellow solid in a yield of 77%. ^{1}H NMR (400 MHz, $CDCl_3$): δ (ppm) 7.70−7.82 (m, 8H), 7.50−7.68 (m, 24H), 7.30−7.46 (m, 6H), 7.27 (d, J = 16.2 Hz, 2H), 7.18 (d, J = 16.1 Hz, 2H), 7.18 (S, 4H), 1.82−2.30 (m, 16H), 0.55−1.02 (m, 84H), 0.25−0.40 (m, 12H). Molecular weight calcd for $C_{130}H_{158}$: 1719.2. MALD/I TOF MS (dithranol) m/z ($[M]^+$): 1720.2. Anal. Calcd for $C_{130}H_{158}$: C, 90.74; H, 9.26. Found: C, 90.70; H, 9.60.

1,4-Bis[2-[4-[2-(9,9-bis(2-ethylhexyl)-9′,9′,9″,9″-tetrakis-(2-methylbutyl)-2,2′;7′,2″-terfluoren-7-yl)ethenyl]phenyl]-ethenyl]benzene (OF-6). The procedure for the synthesis of **OF-5** was followed to prepare **OF-6** from **17c** and **22** as a yellow solid in a yield of 70%. ^{1}H NMR (400 MHz, $CDCl_3$): δ (ppm) 7.50−7.88 (m, 44H), 7.31−7.46 (m, 6H), 7.28 (d, J = 16.3 Hz, 2H), 7.18 (d, J = 16.1 Hz, 2H), 7.18 (s, 4H), 1.90−2.30 (m, 24H), 0.60−1.10 (m, 108H), 0.30−0.50 (m, 24H). Molecular weight calcd for $C_{176}H_{214}$: 2327.7. MALD/I TOF MS (dithranol) m/z ($[M]^+$): 2328.5. Anal. Calcd for $C_{176}H_{214}$: C, 90.74; H, 9.26. Found: C, 90.61; H, 9.48.

1,4-Bis[2-[4-[2-[4-[2-(9,9-bis(2-ethylhexyl)-9′,9′,9″,9″-tetrakis(2-methylbutyl)-2,2′;7′,2″-terfluoren-7-yl)ethenyl]-phenyl]ethenyl]phenyl]ethenyl]-2-cyano-benzene (OF-7). Into a mixture of **21** (0.520 g, 0.422 mmol), [(2-cyano-1,4-phenylene) bis(methylene)]bis-phosphonic acid tetraethyl ester (**23**, 0.085 g, 0.211 mmol) in THF (10.0 mL) was added potassium *t*-butoxide (1.0 M in THF, 0.60 mL, 0.60 mmol) dropwise at 0 °C. The reaction mixture was stirred at room temperature for 2 h and then poured into a large amount of water for extraction with methylene chloride. The organic extracts were washed with brine for drying over $MgSO_4$. When the solvent had evaporated off, the residue was purified with column chromatography on silica gel with petroleum ether/chloroform (1:1 then 1:2) as the eluent to yield **OF-7** (0.374 g, 69%) as a yellow orange solid. ^{1}H NMR (400 MHz, $CDCl_3$): 7.60−7.90 (m, 30H), 7.29−7.50 (m, 27H), 6.80−7.28 (m, 12H), 1.90−2.40 (m, 24H), 0.54−1.10 (m, 108H), 0.30−0.50 (m, 24H). Molecular weight calcd for $C_{193}H_{225}N$: 2558.9. MALD/I TOF MS (dithranol) m/z ($[M]^+$): 2559.9. Anal. Calcd for $C_{193}H_{225}N$: C, 90.59; H, 8.86; N, 0.55. Found: C, 90.58; H, 9.04; N, 0.55.

4,7-Bis[2-[4-[2-[4-[2-(9,9-bis(2-ethylhexyl)-9′,9′,9″,9″-tetrakis(2-methylbutyl)-2,2′;7′,2″-terfluoren-7-yl)ethenyl]-phenyl]ethenyl]phenyl]ethenyl]-2,1,3-benzothiadiazole (OF-8). The procedure for the synthesis of **OF-5** was followed to prepare **OF-8** from **17c** and **24** as a red orange solid in a yield of 72%. ^{1}H NMR (400 MHz, $CDCl_3$): δ (ppm) 7.94 (d, J = 15.5 Hz, 2H), 7.00−7.90 (m, 66H), 1.90−2.80 (m, 24H), 0.50−1.10 (m, 108H), 0.30−0.49 (m, 24H). Molecular weight calcd for $C_{192}H_{224}N_2S$: 2592.0. MALD/I TOF MS (dithranol) m/z ($[M]^+$): 2592.9. Anal. Calcd for $C_{192}H_{224}N_2S$: C, 88.97; H, 8.71; N, 1.08; S, 1.24. Found: C, 88.64; H, 8.79, N, 1.09.

Molecular Structures, Morphology, and Thermal Transition Temperature. ^{1}H NMR spectra were acquired in $CDCl_3$ with an Avance-400 spectrometer (400 MHz). Elemental analysis was carried out by Quantitative Technologies, Inc. Molecular weights were measured with a TofSpec2E MALD/I TOF mass spectrometer (Micromass, Inc., UK). Thermal transition temperatures were determined by differential scanning calorimetry (Perkin-Elmer DSC-7) with a continuous N_2 purge at 20 mL/min. Before taking the reported second heating scans at 20 °C/min, samples were preheated to 350 °C for **OF-1−3** and 320 °C for **OF-4−8**, the upper temperature limits to avoid thermal decomposition, with subsequent cooling at −20 °C/min to −30 °C. Morphology and the nature of phase transition were characterized with a polarizing optical microscope (DMLM, Leica, FP90 central processor and FP82 hot stage, Mettler Toledo).

Absorption and Fluorescence Spectra in Dilute Solution. Dilute solutions of oligofluorenes in toluene were prepared at a concentration of 10^{-6} to 10^{-7} M. Absorption spectra were gathered with an HP 8453E UV−vis−NIR diodes array spectrophotometer. Fluorescence spectra were collected with a spectrofluorimeter (Quanta Master C-60SE, Photon Technology International) at an excitation wavelength of 370 nm in a 90° orientation. Photoluminescence quantum yield standards, Pyrromethene 546 and Rhodamine 590 (Exciton, Inc.), were used as received. Oxygen was removed from solvents by bubbling dry argon with three freeze−pump−thaw cycles at a vacuum level of 10^{-3} Torr. Dilute solutions of Pyrromethene 546 in methanol and Rhodamine 590 in ethanol were prepared at concentrations of 10^{-6} M such that absorbance values of less than 0.1 were obtained at an excitation wavelength of 500 nm. Dilute solution of Rhodamine 590 was assigned a widely accepted value of 0.99.[38] The photoluminescence quantum yield of Pyrromethene 546 in solution was determined with the following formula:

$$\frac{\Phi_{PL,s}}{\Phi_{PL,r}} = \frac{1 - 10^{-A_r}}{1 - 10^{-A_s}} \frac{B_s \overline{n_s^2}}{B_r \overline{n_r^2}} \tag{1}$$

where subscripts s and r refer, respectively, to sample and reference; A denotes absorbance at the excitation wavelength, B is the integrated intensity across the entire emission spectrum, and $\overline{n^2}$ is defined as follows:

$$\overline{n^2} \equiv \frac{\int I(\lambda) n^2(\lambda) \mathrm{d}\lambda}{\int I(\lambda) \mathrm{d}\lambda} \tag{2}$$

in which $I(\lambda)$ stands for emission intensity, $n(\lambda)$ is the refractive index dispersion of the solvent,[39] and the integration was performed over the entire spectrum. The result for the Pyrromethene 546 solution, Φ_{PL}= 0.96 ± 0.03, agrees with the reported value of 0.99,[40] thus validating the experimental procedure. An excitation wavelength of 450 nm was used for dilute solutions of **OF-1−8** and Pyrromethene 546 for the measurement of quantum yield. In general, the presently reported Φ_{PL} values are accompanied by an uncertainty of ±2% of the mean value.

Preparation and Characterization of Neat Films. Optically flat fused silica substrates were coated with a thin film of PEDOT/PSS (Baytron P VP AI 4083, Bayer) alignment layer and uniaxially rubbed. Films of **OF-1−8** were prepared by spin-coating from 1.8 wt % solution in toluene at 4000 rpm followed by drying in a vacuum overnight. Thermal annealing was performed in dry argon purged glassware at temperatures 10−15 °C above T_g for 25 to 30 min. A UV−vis−NIR spectrophotometer (Lambda-900, Perkin-Elmer) with a linear polarizer (H′NPB, Polaroid) was used to characterize linear dichroism. Photoluminescence was characterized using the spectrofluorimeter with a liquid light guide directing unpolarized excitation at 370 nm onto the sample film at normal incidence. Films for electron diffraction (JEM 2000 EX,

(38) Beaumont, P. C.; Johnson, D. G.; Parsons, B. J. *J. Chem. Soc., Faraday Trans.* **1993**, *89*, 4185.

(39) Washburn, E. W., Ed. *International Critical Tables of Numerical Data, Physics, Chemistry and Technology*, Vol. VII; McGraw-Hill: New York, 1930.

(40) Shah, M.; Thangaraj, K.; Soong, M.-L.; Wolford, L. T.; Boyer, J. H. *Heteroatom. Chem.* **1990**, *1*, 389.

JEOL USA) were prepared following the same procedures except on single crystalline sodium chloride substrates. These films were floated off in a trough filled with deionized water for mounting onto copper grids.

Preparation and Characterization of Linearly Polarized OLEDs. A conductive PEDOT/PSS alignment layer and films of **OF-1**, **2**, and **6** were prepared as described above on ITO-patterned substrates. After consecutive depositions of TPBI and LiF at 0.4 and 0.1 nm/s, the cathode was applied by co-depositing magnesium and silver at 1.00 and 0.05 nm/s, respectively. Sublimation of all materials was conducted at a vacuum level of 10^{-6} Torr or higher. After encapsulation in a dry nitrogen glovebox, the OLEDs were characterized using a Keithley 2400 source/measure unit and a PhotoResearch PR650 spectroradiometer capable of polarization analysis. Polarization analysis of both photo- and electroluminescence was performed using a pair of linear polarizers.

Acknowledgment. We are grateful for the financial support provided by the Multidisciplinary University Research Initiative, administered by the Army Research Office, under DAAD19-01-1-0676, the National Science Foundation under Grant CTS-0204827, Eastman Kodak Company, and the New York State Center for Electronic Imaging Systems. Additional funding was provided by the Department of Energy Office of Inertial Confinement Fusion under Cooperative Agreement DE-FC03-92SF19460 with the Laboratory for Laser Energetics and the New York State Energy Research and Development Authority. The support of DOE does not constitute an endorsement by DOE of the views expressed in this article.

Supporting Information Available: Procedures for the synthesis and purification of intermediates, spectra of UV−vis absorption and photoluminescence with an unpolarized excitation at 370 nm in both dilute solution and glassy-nematic film (pdf). These materials are available free of charge via the Internet at http://pubs.acs.org.

CM034579M